Journal of The Electrochemical Society, **164** (2) A518-A523 (2017)
0013-4651/2017/164(2)/A518/6/$37.00 © The Electrochemical Society

In Situ Infrared Spectroscopy Study of $PYR_{14}TFSI$ Ionic Liquid Stability for Li–O_2 Battery

Nataliia Mozhzhukhina, Alvaro Y. Tesio,* Lucila P. Mendez De Leo, and Ernesto J. Calvo[z]

INQUIMAE-CONICET-Facultad de Ciencias Exactas y Naturales, Universidad de Buenos Aires Ciudad Universitaria, Buenos Aires 1428, Argentina

In situ infrared subtractive normalized Fourier transform infrared spectroscopy (SNIFTIRS) experiments were performed simultaneously with the electrochemical experiments relevant to Li-air battery operation on gold cathodes in ionic liquid $PYR_{14}TFSI$ based electrolyte. Ionic liquid anion was found to be stable, while the cation PYR_{14}^+ was found to decompose in studied conditions. In oxygen saturated LiTFSI containing $PYR_{14}TFSI$ electrolyte carbon dioxide and water were formed at potential 4.3 V either with or without previous oxygen electro-reduction reaction. However in deoxygenated LiTFSI contacting ionic liquid no formation of CO_2 or water was observed, suggesting oxygen presence to be crucial in carbon dioxide production.
 [DOI: 10.1149/2.1391702jes]

Manuscript submitted November 22, 2016; revised manuscript received December 27, 2016. Published January 18, 2017.

In the recent years scientific community worldwide has shown an enormous research interest for the development of non-aqueous Li-air battery technology due to its high theoretical energy density.[1–18] A stable electrolyte still remains one of the biggest challenges to resolve for improving a durability of the battery. While the majority of research effort has focused on organic solvents (initially alkyl carbonates, and later ethers, acetonitrile and dimethyl sulfoxide), there has been also some interest in the use of ionic liquids as electrolyte for the Li-oxygen system.

Ionic liquids (ILs) are organic salts that are liquid at room temperature and posses a set of unique properties: non volatility, high oxygen solubility, non flammability and high stability that make them promising candidates as electrolyte for metal-air, and particularly Li-air batteries.[19,20] One of the most available and widely investigated ILs for lithium batteries is N-butyl-N-methylpyrrolidinium bis(trifluoromethanesulfonyl)amide (possible abbreviations for the cation are: BMP^+, C_4mpyr^+, PYR_{14}^+, Pyr_{14}^+ and for the anion are: $TFSI^-$, $[NTf2]^-$ or $[N(SO_2CF_3)_2]^-$). In this publication will use $PYR_{14}TFSI$ abbreviation.

It has been shown that in many ionic liquids, including $PYR_{14}TFSI$, in the absence of protons and metal ions, reversible formation of O_2/O_2^- couple is observed,[21–27] an analogous behavior as in the solutions of tetralkyl ammonium salts in organic solvents.

However, the chemistry of ORR in ionic liquids changes in the presence of metal ions, and especially in the presence of the small Lewis acid Li^+ cation. De Giorgio et al.[28] have reported that addition of LiTFSI to $PYR_{14}TFSI$ up to of 25 mM concentration did not modify the GC electrode response, and a further increase of the Li^+ amount above that value caused a gradual distortion of the oxygen reduction reaction (ORR) cyclic voltammetry (CV) curves. In 0.1 M Li^+ the oxygen reduction current was lowered and ORR became electrochemically irreversible in several ionic liquids. Allen et al.[29,30] have studied ORR in two ionic liquids EMITFSI and $PYR_{14}TFSI$ in the presence of Li^+, Na^+, K^+ and TBA^+ cations and have found a strong correlation between the ORR products and the ionic charge density of the cations. They explained these results based on Hard Soft Acid Base (HSAB) theory and correlated the reaction mechanism with the acidity of the cations and the basicity of the ORR products, i.e. O_2^-. For the $PYR_{14}TFSI$ in 25 mM Li^+ the authors described the ORR as follows:

$$Li^+ + O_2 + e \rightarrow LiO_2 \quad [1]$$

$$2LiO_2 \rightarrow Li_2O_2 + O_2 \quad [2]$$

$$PYR_{14}^+ + O_2 + e \rightarrow PYR^+ - O_2^- \quad [3]$$

And following for the oxygen evolution reaction (OER):

$$PYR^+ - O_2^- \rightarrow PYR_{14}^+ + O_2 + e \quad [4]$$

$$LiO_2 \rightarrow Li^+ + O_2 + e \quad [5]$$

$$Li_2O_2 \rightarrow 2Li^+ + O_2 + 2e. \quad [6]$$

Lodge et al. have also reported a detailed characterization of the reduction of the ORR in pure $PYR_{14}TFSI$: reversible reduction of O_2 to O_2^- and O_2^- to O_2^{2-} take place at potentials 2.1 V and 0.8 V vs. Li^+/Li, respectively. They found that in the presence of very low concentration of Li^+ such as 1 mM, the ORR take place in two distinct peaks: 2.5 V (involving O_2 and Li^+) and 1.9 V (involving PYR^+ and O_2). However, at higher Li^+ concentration, i.e. 0.3 M the ORR starts at the same potential as for low Li^+ concentration and leads to complete electrode passivation by insoluble Li_2O_2, estimated to be 7 monolayers of a uniform film.[31]

Herranz et al. have used the Rotating Ring Disc Electrode (RRDE) experiments to quantify the stability of $PYR_{14}TFSI$ in the presence of superoxide anion and estimated the rate constant of the reaction to be three orders of magnitude less than that for propylene carbonate (PC).[32] Fritz and co-workers used in-situ Raman spectroscopy to detect the products of oxygen reduction in 1-ethyl-3-methylimidazolium bis(trifluoromethyl sulfonyl)imide $C_2mimTFSI$ and $Pyr_{14}TFSI$.[33] They reported that $C_2mimTFSI$ degrades during the reduction of oxygen, while $PYR_{14}TFSI$ was found to be resistant to degradationin 10 mM LiTFSI being superoxide the first reaction product and Li_2O_2 further formed.

Up to date there are a handful of publications that report testing of some ionic liquids, mostly $PYR_{14}TFSI$ in Li-air charge-discharge experiments. In 2005 Kuboki et al. reported a Li-air battery using ionic liquid electrolyte, however only the first discharge cycle was reported without recharging cycle.[34] In 2014 Elia et al. reported an advanced Li-air battery based of $PYR_{14}TFSI$-LiTFSI electrolyte; they claimed the battery to have a stable electrode-electrolyte interface, highly reversible charge−discharge cycling behavior and low charge overpotential.[35] On the other hand, Piana et al. have investigated three different setups for a Li-O_2 battery with $PYR_{14}TFSI$ based electrolyte: one-compartment Li-O_2 cell with metallic Li as anode, two-compartment cell with propylene carbonate (PC) as anode electrolyte with Li-ion conducting solid separator, and one-compartment cell with lithiated $Li_4Ti_5O_{12}$ (LTO) as anode. For the first configuration it was found that pyrrolidinium ion is reduced on metallic lithium, producing substantial amounts of alkenes and amines. The cell with lithiated LTO did solve the problem observed with metallic lithium, however it showed poor cyclability, therefore the authors suggested that $PYR_{14}TFSi$ might not have enough long-term stability against ORR products.[36]

In situ IR spectroscopy is a very useful and versatile tool that allows to detect species formed at each applied potential. To the best of

*Electrochemical Society Student Member.
[z]E-mail: calvo@qi.fcen.uba.ar

our knowledge, this technique has been used twice to study solvent decomposition in Li-O_2 system. In 2013 our group has used in-situ infrared subtractive normalized Fourier transform infrared spectroscopy (SNIFTIRS) to study the stability of DMSO under conditions relevant to Li-air battery operation.[37] More recently, Hardwick and co-workers have employed in-situ attenuated total reflectance surface enhanced infrared absorption spectroscopy (ATR-SEIRAS) to elucidate superoxide induced ring opening in propylene carbonate electrolyte.[38]

In the present work, in situ infrared spectroscopy experiments were performed simultaneously with electrochemical experiments and complemented by differential electrochemical mass spectrometry (DEMS), to investigate the PYR_{14}TFSI-based electrolyte stability under conditions relevant to the Li−air cell operation. While DEMS detects electrolyte decomposition products in the gas phase, in-situ SNIFTIRS allows detection of the decomposition products in the solvent phase, adjacent to the electrode surface.

Experimental

Chemicals and Solutions.—Anhydrous N-butyl-N-methylpyrrolidinium bis(trifluoromethane-sulfonyl) amide (PYR_{14}TFSI, Io-Li-Tec), Bis(trifluoromethane)sulfonimide lithium salt (544094, LiTFSI, sigma aldrich) and Metallic lithium wire, diam. 3.2 mm, 99.9% trace metals basis (220914, Sigma Aldrich), were stored in the argon-filled MBRAUN glove box with an oxygen content $\leq$0.1 ppm and water content below 2 ppm. PYR_{14}TFSI and in mixture with LiTFSI were dried for several hours at 80°C under vacuum. All solutions were prepared inside the glove box, and the water content was measured using the Karl Fisher 831 KF Coulometer (Metrohm). Solutions were found to contain around 20 ppm of water.

Potentiometric Experimental.—The reference $Li_2Mn_2O_4$/$LiMn_2O_4$ electrode was prepared as described: 1) $LiMn_2O_4$ synthesis: Li_2CO_3 and MnO_2 were mixed in a molar relation 0.51:2, grounded, pressed and heated at 350 °C for 12 h and at 800 °C for 24 h. 2) $Li_2Mn_2O_4$ synthesis: equimolar amounts of $LiMn_2O_4$ and LiI were mixed and placed in a vacuum oven at 80 °C overnight. 3) Equimolar quantities of $LiMn_2O_4$ and $Li_2Mn_2O_4$ were mixed with Carbon black (10% of total mixture weight) and PVDF binder (10% of total mixture weight) and dissolved in an appropriate organic solvent to make an ink. 4) A Pt wire was covered with the ink, and placed in a fritted glass compartment containing 0.1 M LiTFSI in PYR_{14}TFSI. The reference electrode was calibrated inside of glove box with respect to Li/Li^+ couple, which is commonly used as a reference in Li−air battery studies.

Infrared Experimental.—Electrochemical in situ subtractively normalized interfacial Fourier transform infrared spectroscopy (SNIFTIRS) experiments were carried out on a Thermo Nicolet 8700 (Nicolet, Madison, WI) spectrometer equipped with a custom-made external tabletop optical mount, an MCTA detector, and a custom-made Teflon electro-chemical cell (Scheme 1) with a polycrystalline gold disc electrode aligned against the CaF_2 window, a 1 in. (25 mm) CaF_2 equilateral prism (Harrick Scientific Technology). Typically, a few micrometers of electrolyte solution separated the electrode and the CaF_2 window. The design of spectroelecrochemcal cells for FTIRS or PMIRRAS have been described before in the literature.[39,40] The electrochemical cell was a conventional three-electrode cell connected to a Jaissle IMP88 Potentiostat controlled by the computer via a digital-to-analog converter (Agilent USB AD/DA converter). All potentials were measured with respect to a non aqueous $Li_2Mn_2O_4$/$LiMn_2O_4$ reference electrode (as described above) and a Pt foil used as counter electrode. The working gold electrode has been polished first with 1 μm alumina, then with 0.3 μm and finally 0.05 μm alumina, untill mirror like appearance has been achieved. The electrode potential was varied from 3.0 to 2.2 V and back to 4.2 V .Each potential step comprises an equilibration time of 120 s followed by the acquisition of the spectrum by averaging 200 scans at 4 cm^{-1} resolution. For

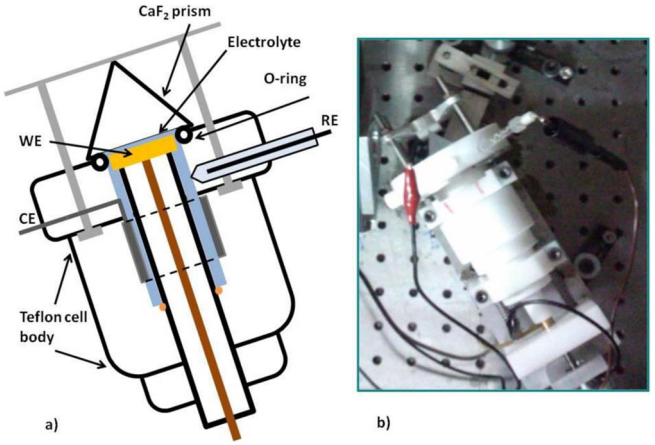

Scheme 1. Experimental spectroelectrochemical cell a) schematic representation and b) photograph. WE: working electrode, CE: counter electrode, RE: reference electrode.

each system, a spectrum was obtained at open circuit and taken as reference. In a typical in situ FTIR spectroscopy experiment, it is necessary to measure a reference spectrum at a potential, where the electrochemical process does not take place, and a sample spectrum, where the desired process does take place. A ratio of the two spectra is then obtained. This type of experiment was originally called subtractively normalized interfacial Fourier transform infrared spectroscopy (SNIFTIRS). In SNIFTIRS spectra, usually there are bands in both the up and down directions with respect to the baseline. Taking R_0 as the reflectance in the reference spectrum and R as the sample spectrum reflectance, positive bands ($R_0 > R$) correspond to consumption of species and negative bands ($R_0 < R$) correspond to appearance of new species. Transmission spectra of the solutions were performed using a thin optical pass liquid cell with CaF_2 windows. The resolution was set to 4 cm^{-1}, and 200 scans were performed.

All received spectra were processed with the OMNIC software in the following manner: standard gaseous water and carbon dioxide spectra were subtracted separately from each obtained spectrum in order to eliminate noise corresponding to ambient air.

Differential electrochemical mass spectrometry (DEM).—DEM was accomplished using a Pfeiffer vacuum Omnistar GSD 320 gas analysis system with a quadrupole mass spectrometer QGM 220 (mass range 1−200 amu) with ion gastight ion source, yttriated iridium-filament with secondary electron multiplier C-SEM and Faraday detectors. The DEMS cell setup was a modification of the design pioneered by Baltruschat et al.[41,42] and consisted of a stainless steel base with a PTFE body. A gold sputtered PTFE membrane gas diffusion electrode (200 μm thick and 0.1 μm pore diameter T01047WPH Microclar Teflon) with 0.50 cm^2 geometric electroactive area located at the bottom of the cell. The Au sputtered membrane was mechanically supported on a porous stainless steel frit. Surface tension of electrolyte prevents penetration in the capillary porous structure of the PTFE membrane. The electrolyte-vacuum interface was connected to the gas analyzer by 1/16″ ss tubing through a Varian precision needle valve adjusted at 2×10^{-6} mbar. A nonaqueous $LiMn_2O_4$/$LiMn_2O_4$ reference electrode in the same electrolyte was used in a fritted glass compartment and a 1 cm^2 platinum gauze (Johnson Matthey) was employed as counter electrode.

Results and Discussion

Cyclic voltammetry of oxygen saturated ionic liquid PYR_{14}TFSI containing 25 mmol LiTFSI is depicted on the Figure 1. Two reduction peaks are observed at 2.15 and 1.9 V, that could be assigned to oxygen reduction to superoxide involving Li^+ and PYR_{14}^+ respectively. On the reverse scan, the first oxidation peak corresponds to the

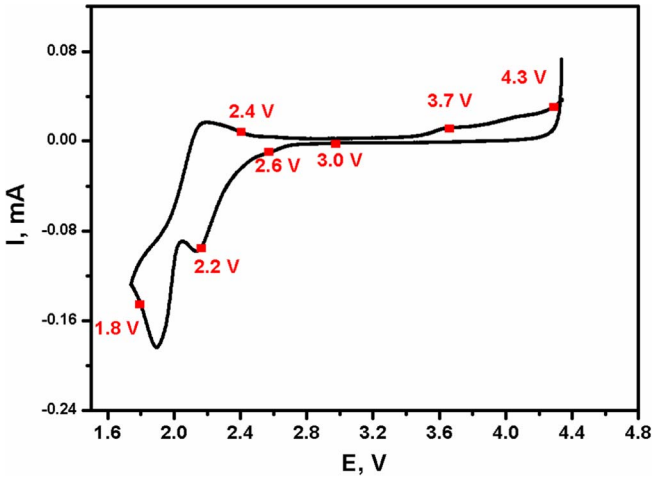

Figure 1. Cyclic voltammetry of 0.2 cm^2 Au electrode in 25 mM LiTFSI in O_2 saturated PYR_{14}-TFSI, scan rate 50 mV/s.

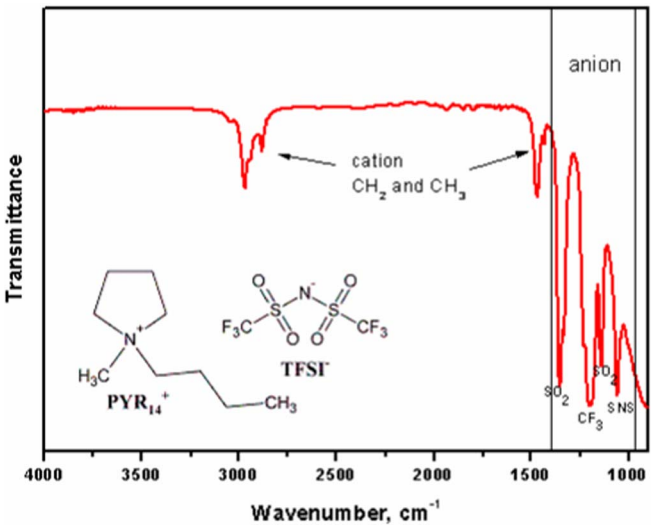

Figure 3. IR Spectrum and structure of PYR_{14}TFSI ionic liquid.

oxygen evolution from superoxide stabilized by ionic liquid cation (PYR_{14}^+ - O_2^-), while oxidation of lithium peroxide formed by LiO_2 disproportionation is observed at much higher potentials above 3.5 V, in agreement with previous studies.[29,31]

Results of differential electrochemical mass spectrometry (DEMS) performed simultaneous to the ORR (1.8 V) and OER (2.4–4.5 V) in pure ionic liquid and 25 mM LiTFSI in PYR_{14}TFSI are shown in Figure 2.

In both systems oxygen consumption is observed at 1.8 V. However oxygen evolution for pure ionic liquid occurs at 2.4 V, while for the 25 mM Li^+ salt in the ionic liquid, oxygen evolution takes place at two distinct potentials: 2.4 and 4.5 V respectively. Those results are in agreement with a previous research and confirm oxygen evolution from the superoxide in the case of pure ionic liquid, and oxygen evolution partly from superoxide and lithium peroxide in the case of Li^+ salt containing ionic liquid. Ionic currents for mass 44 at potential of 4.5 V demonstrate the formation of carbon dioxide by decomposition of the ionic liquid in both electrolytes.

The IR spectrum of the ionic liquid under study exhibits several peaks in the 4000–900 cm^{-1} interval. The spectrum and molecular structure of pure PYR_{14}TFSI is shown in Figure 3 and the assignment of the peaks is summarized in Table I. Both the spectrum and assignments are in perfect agreement with previously reported IR data for similar systems.[43–45]

In order to evaluate the stability of the ionic liquids under conditions relevant to the Li-air battery operation, a set of fixed potentials has been applied to the Au cathode and the IR spectra have been collected at each potential. The potentials applied were chosen as indicated in the cyclic voltammetry of oxygen saturated 25 mM LiTFSI in PYR_{14}TFSI solution depicted in Figure 1, as well as previously reported data on charge-discharge experiments in similar systems.

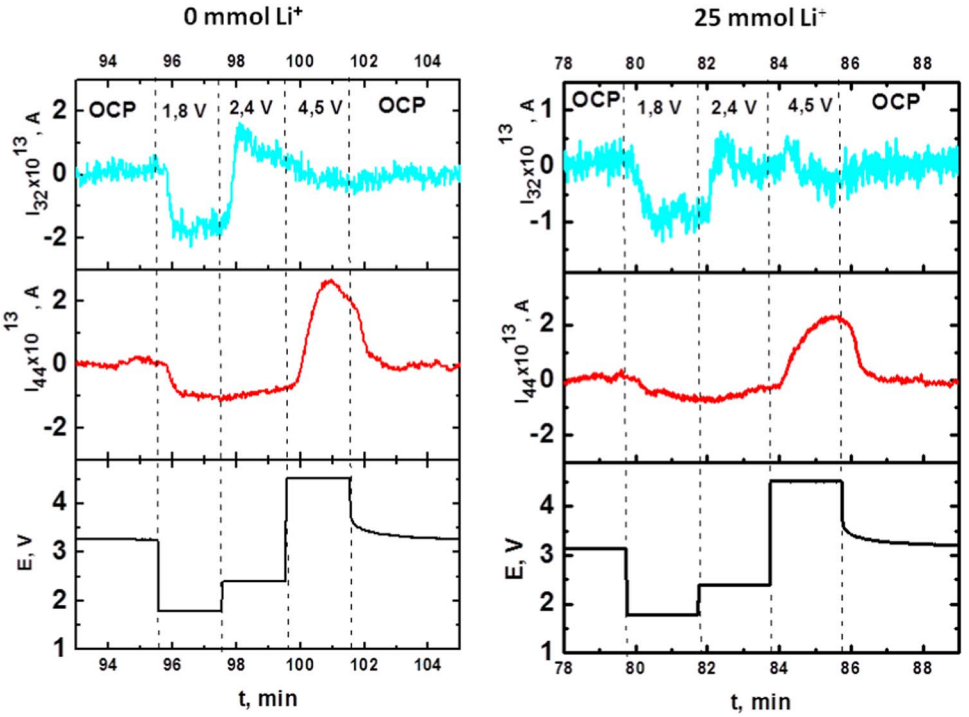

Figure 2. DEMS ionic currents for mass 32 and 44 respectively in O_2 saturated solution of 25 mM LiTFSI in PYR_{14}-TFSI at different potentials: OCP, 1.8, 2.4, 4.5 V and OCP.

Table I. Peak assignments for the ionic liquid $PYR_{14}TFSI$.

Wavenumber, cm^{-1}	Assignment	
2970	CH_3 antisymmetric C-H stretching ($\nu_{as}CH_3$)[48]	cation
2943	CH_2 antisymmetric stretching ($\nu_{as}CH_2$)[48]	cation
2882	CH_3 symmetric C-H stretching ($\nu_{s}CH_3$)[48]	cation
1467	CH_2 scissoring bending ($\delta_{s}CH_2$)[48]	cation
1433	CH_3 antisymmetric bending ($\delta_{as}CH_3$)[48]	cation
1353	SO_2 antisymmetric stretching ($\nu_{as}SO_2$)[48]	anion
1195 broad peak	CF_3 antisymmetric stretching ($\nu_{as}CF_3$)[48,49]	anion
1225 shoulder		
1138	SO_2 symmetric stretching ($\nu_{s}SO_2$)[48]	anion
1056	SNS asymmetric stretching ($\nu_{as}SNS$)[49]	anion

We first analyzed the system at near open circuit potential (about 3.0 V), then during ORR (2.2 V), back near open circuit potential (3.0 V), during OER (3.7, 4.3 and 4.9 V respectively), and then back to reducing potential of 2.2 V.

In the SNIFTIR spectra, negative peaks (downward) correspond to the compounds that are formed, while positive peaks (upward) correspond to the modes that disappear.

The spectra obtained in the oxygen saturated 25 mM LiTFSI solution in PYR_{14}-TFSI are shown on the Figure 4. Almost in all spectra positive peaks at 2970, 2943, 2882, 1467 and 1433 cm^{-1} are detected with higher intensity at 3.7, 4.3 and 4.9 V. Those are attributed to CH_2 and CH_3 groups of ionic liquid cation PYR^+, thus suggesting slow decomposition of ionic liquid cation during ORR and more pronounced decomposition during the OER at higher oxidizing potentials.

Notably, at the high oxidizing potential of 4.3 and 4.9 V a downward peak is detected at 2340 cm^{-1} that corresponds to the formation of CO_2 at the electrode surface.[46] Those results are consistent with data obtained from DEMS, showing CO_2 evolution at 4.5 V. An important result is that by switching back to 2.2 V, the peak intensity seems unchanged. Thus we suggest that the CO_2 is formed during the recharge starting at 4.3 V which cannot be reduced neither undergoes reaction with lithium peroxide deposit during the following discharge.

Also at 4.9 V two broad negative peaks appear approximately at 3470 and 1720 cm^{-1}. They may be assigned to the formation of water at the interface (the shift of one of the peaks to more positive wave numbers could be explained in terms of water environment and high positive potential). Interestingly, in the following discharge (step to 2.2 V), those two peaks disappear.

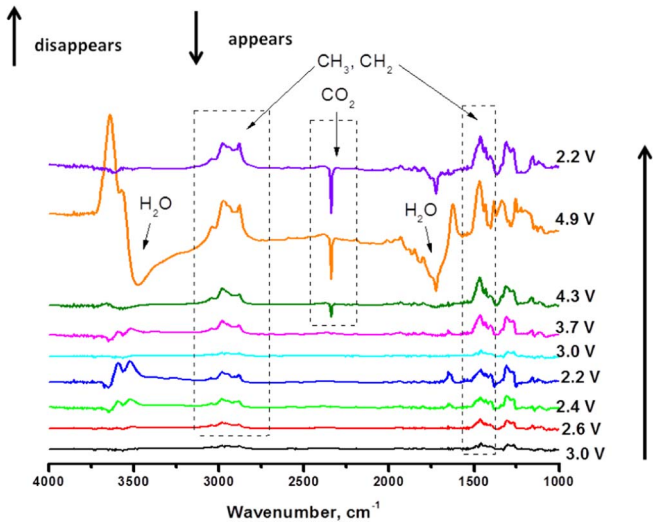

Figure 4. In situ IR spectra taken in O_2 saturated 25 mM LiTFSI in $PYR_{14}TFSI$ solution on Au working electrode.

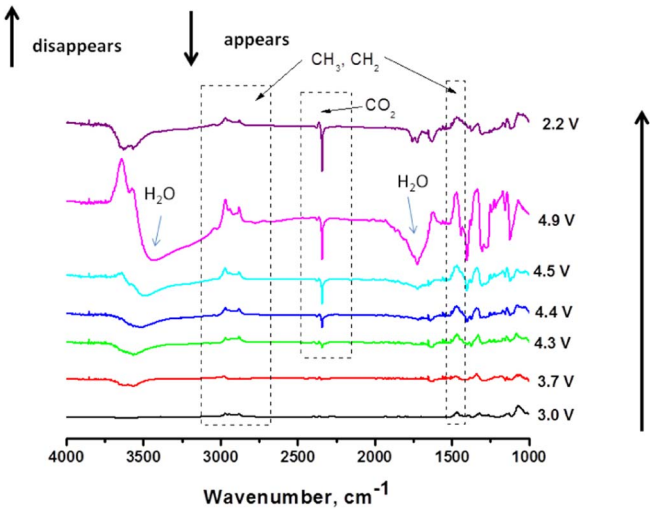

Figure 5. In situ IR spectra taken in O_2 saturated 25 mM LiTFSI solution in $PYR_{14}TFSI$ on Au working electrode, at potentials above 3.0 V.

We can conclude that during the recharge, the ionic liquid cation undergoes decomposition forming carbon dioxide and water, and water formed during ionic liquid decomposition, is consumed during the following battery discharge, probably reacting with lithium peroxide to form lithium hydroxide and hydrogen peroxide.

$$Li_2O_2 + 2H_2O \rightarrow H_2O_2 + 2LiOH \quad [7]$$

To discover, whether the presence of lithium superoxide or peroxide promoted the decomposition of the PYR^+ cation, we have repeated the experiment, but avoiding the ORR excursion (2.6, 2.4 and 2.2 V). The resulting spectra are plotted in Figure 5 and differ very slightly from those reported previously.

From 4.3 V, a negative peak at 2340 cm^{-1} is observed which corresponds to carbon dioxide formation. At 4.5 V broad negative peaks at 3470 and 1720 cm^{-1} indicate formation of water. Therefore, we can conclude that with or without ORR, the ionic liquid decomposition proceeds in a similar way.

To fully elucidate the mechanism for PYR^+ decomposition and CO_2 formation, analogous experiments were performed on the deoxygenated $PYR_{14}TFSI$ in the presence of Li^+ ion (Figure 6) and on the pure deoxygenated ionic liquid without Li^+ (Figure 7).

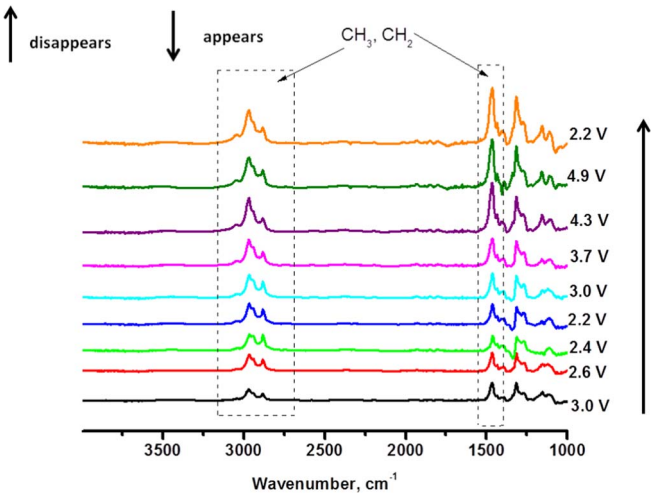

Figure 6. In situ IR spectra taken in deoxygenated 25 mM LiTFSI solution in $PYR_{14}TFSI$ on Au working electrode.

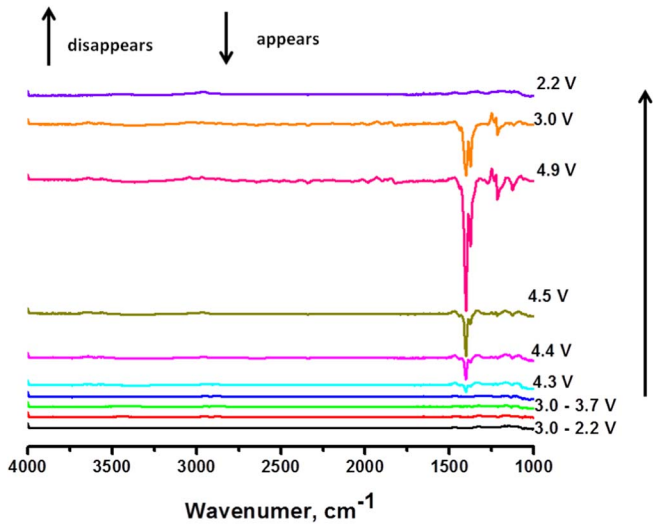

Figure 7. In situ IR spectra taken in O_2 free $PYR_{14}TFSI$ ionic liquid on Au working electrode.

Figure 6 shows positive peaks at 2970, 2943, 2882, 1467 and 1433 cm^{-1} independently of the applied potential. These features are to be attributed to the ionic liquid PYR^+ cation decomposition as described previously and this decomposition process in the presence of Li^+ ion is independent of the applied potential.

The results obtained from pure deoxygenated ionic liquid (Figure 7) do not show any peaks corresponding to PYR^+ decomposition, thus corroboration our assumption that the Lewis acid Li^+ alone is responsible for the slow ionic liquid decomposition. However, at potentials of 4.3 V and 4.4 V downward peaks at near 1400 cm^{-1} and 1375 cm^{-1}, respectively, appear. Those peaks grow while increasing the applied potential, and decrease while switching back to 3.0 V with complete disappearance at 2.2 V. Considering the reversibility of this phenomena, we assume that those peaks represent changes in the electrical double layer due to the adsorption of the ionic liquid anion species, probably by SO_2 groups, at high positive potential.[47]

Notably, in Figures 6 and 7 no peak appears at 2340 cm^{-1} wave number, as well as no peaks are seen at 3470 and 1720 cm^{-1}. Those results imply that no carbon dioxide, neither water were formed under those anaerobic conditions in the absence of lithium ions. It is fair to conclude that the presence of O_2 in the solution is necessary to produce in CO_2 and H_2O.

Conclusions

In this paper the stability of the ionic liquid PYR_{14}-TFSI has been evaluated under conditions relevant for the Li-air battery operation.

In situ SNIFTIRS experiments have indicated relative stabilty of the ionic liquid anion, while the cation $PYR_{14}{}^+$ showed several possible decomposition reactions under the studied conditions.

We showed carbon dioxide and water formation starting at 4.3 V in oxygen saturated LiTFSI containing ionic liquid, which is in agreement with results obtained by DEMS, indicating carbon dioxide evolution at 4.5 V. Importantly, carbon dioxide and water were formed regardless of oxygen reduction reaction was occurring or not.

Interestingly, oxygen free solutions have shown neither water nor carbon dioxide formation, suggesting that the presence of oxygen is crucial for those parasitic reactions to take place.

The present results are of importance to estimate ionic liquid PYR_{14}-TFSi stability for its possible use in Li-air battery cathodes. We have shown that this ionic liquid could be relatively stable until the charging voltage of 4.3 V. As in the case with other solvents (as DMSO for example), the charging potential can be lowered with redox mediators if necessary. However more experimental evidence is required to conclude if $PYR_{14}TFSI$ ionic liquid is an adequate electrolyte for Li-air battery.

Acknowledgments

Funding from UBA, CONICET and ANPCyT PICT 2014V No. 36542 are gratefully acknowledged. NM has a doctoral fellowship and A.Y.T a postdoctoral fellowship form CONICET which are gratefully acknowledged.

References

1. L. Grande, E. Paillard, J. Hassoun, J. B. Park, Y. J. Lee, Y. K. Sun, S. Passerini, and B. Scrosati, "The lithium/air battery: still an emerging system or a practical reality?" *Adv Mater*, **27**, 784 (2015).
2. Z. Ma, X. Yuan, L. Li, Z.-F. Ma, D. P. Wilkinson, L. Zhang, and J. Zhang, "A review of cathode materials and structures for rechargeable lithium-air batteries." *Energy & Environmental Science*, **8**, 2144 (2015).
3. R. Van Noorden, "The rechargeable revolution: A better battery." *Nature*, **507**, 26 (2014).
4. N. Imanishi and O. Yamamoto, "Rechargeable lithium–air batteries: characteristics and prospects." *Materials Today*, **17**, 24 (2014).
5. K. Amine, R. Kanno, and Y. Tzeng, "Rechargeable lithium batteries and beyond: Progress, challenges, and future directions." *MRS Bulletin*, **39**, 395 (2014).
6. A. C. Luntz and B. D. McCloskey, "Nonaqueous Li-air batteries: a status report." *Chemical reviews*, **114**, 11721 (2014).
7. J. Lu, L. Li, J. B. Park, Y. K. Sun, F. Wu, and K. Amine, "Aprotic and aqueous Li-O(2) batteries." *Chemical reviews*, **114**, 5611 (2014).
8. B. Scrosati, K. M. Abraham, W. Van Schalkwijk, and J. Hassoun, *Lithium Batteries* 2013.
9. N. Garcia-Araez and P. Novák, "Critical aspects in the development of lithium–air batteries." *Journal of Solid State Electrochemistry*, **17**, 1793 (2013).
10. F. Cheng and J. Chen, "Metal-air batteries: from oxygen reduction electrochemistry to cathode catalysts." *Chemical Society reviews*, **41**, 2172 (2012).
11. L. J. Hardwick and P. G. Bruce, "The pursuit of rechargeable non-aqueous lithium–oxygen battery cathodes." *Current Opinion in Solid State and Materials Science*, **16**, 178 (2012).
12. Z. Peng, S. A. Freunberger, Y. Chen, and P. G. Bruce, "A reversible and higher-rate Li-O2 battery." *Science*, **337**, 563 (2012).
13. N. S. Choi, Z. Chen, S. A. Freunberger, X. Ji, Y. K. Sun, K. Amine, G. Yushin, L. F. Nazar, J. Cho, and P. G. Bruce, "Challenges facing lithium batteries and electrical double-layer capacitors." *Angew Chem Int Ed Engl* **51**, 9994 (2012).
14. J. Christensen, P. Albertus, R. S. Sanchez-Carrera, T. Lohmann, B. Kozinsky, R. Liedtke, J. Ahmed, and A. Kojic, "A Critical Review of Li/Air Batteries." *Journal of the Electrochemical Society*, **159**, R1 (2012).
15. G. Girishkumar, B. McCloskey, A. C. Luntz, S. Swanson, and W. Wilcke, "Lithium-air battery: Promise and challenges." *Journal of Physical Chemistry Letters*, **1**, 2193 (2010).
16. K. M. Abraham, Lithium–Air and Other Batteries Beyond Lithium-Ion Batteries. In *Lithium Batteries*; John Wiley & Sons, Inc., 2013; pp. 161.
17. E. J. Calvo, "The kinetics of oxygen electroreduction: A long way from iron rust to lithium-air batteries." *Materials and Corrosion*, **65**, 345 (2014).
18. D. Sharon, D. Hirshberg, M. Afri, A. Garsuch, A. A. Frimer, and D. Aurbach, "Lithium-oxygen electrochemistry in non-aqueous solutions." *Israel Journal of Chemistry*, **55**, 508 (2015).
19. M. Kar, T. J. Simons, M. Forsyth, and D. R. MacFarlane, "Ionic liquid electrolytes as a platform for rechargeable metal-air batteries: a perspective." *Physical Chemistry Chemical Physics*, **16**, 18658 (2014).
20. D. R. MacFarlane, M. Forsyth, P. C. Howlett, M. Kar, S. Passerini, J. M. Pringle, H. Ohno, M. Watanabe, F. Yan, W. Zheng, S. Zhang, and J. Zhang, "Ionic liquids and their solid-state analogues as materials for energy generation and storage." *Nature Reviews Materials*, **1**, 15005 (2016).
21. I. M. AlNashef, M. L. Leonard, M. A. Matthews, and J. W. Weidner, "Superoxide electrochemistry in an ionic liquid." *Industrial and Engineering Chemistry Research*, **41**, 4475 (2002).
22. M. T. Carter, C. L. Hussey, S. K. D. Strubinger, and R. A. Osteryoung, "Electrochemical reduction of dioxygen in room-temperature imidazolium chloride-aluminum chloride molten salts." *Inorganic Chemistry*, **30**, 1149 (1991).
23. X. J. Huango, E. I. Rogers, C. Hardacre, and R. G. Compton, "The reduction of oxygen in various room temperature ionic liquids in the temperature range 293-318 K: Exploring the applicability of the Stokes-Einstein relationship in room temperature ionic liquids." *Journal of Physical Chemistry B*, **113**, 8953 (2009).
24. R. G. Evans, O. V. Klymenko, S. A. Saddoughi, C. Hardacre, and R. G. Compton, "Electroreduction of oxygen in a series of room temperature ionic liquids composed of group 15-centered cations and anions." *Journal of Physical Chemistry B*, **108**, 7878 (2004).
25. Y. Katayama, H. Onodera, M. Yamagata, and T. Miura, "Electrochemical reduction of oxygen in some hydrophobic room-temperature molten salt systems." *Journal of the Electrochemical Society*, **151**, A59 (2004).
26. Y. Katayama, K. Sekiguchi, M. Yamagata, and T. Miura, "Electrochemical behavior of oxygen/superoxide ion couple in 1-butyl-1-methylpyrrolidinium bis(trifluoromethylsulfonyl)imide room-temperature molten salt." *Journal of the Electrochemical Society*, **152**, E247 (2005).

27. S. Monaco, A. M. Arangio, F. Soavi, M. Mastragostino, E. Paillard, and S. Passerini, "An electrochemical study of oxygen reduction in pyrrolidinium-based ionic liquids for lithium/oxygen batteries." *Electrochimica Acta*, **83**, 94 (2012).
28. F. De Giorgio, F. Soavi, and M. Mastragostino, "Effect of lithium ions on oxygen reduction in ionic liquid-based electrolytes." *Electrochemistry Communications*, **13**, 1090 (2011).
29. C. J. Allen, J. Hwang, R. Kautz, S. Mukerjee, E. J. Plichta, M. A. Hendrickson, and K. M. Abraham, "Oxygen Reduction Reactions in Ionic Liquids and the Formulation of a General ORR Mechanism for Li–Air Batteries." *The Journal of Physical Chemistry C*, **116**, 20755 (2012).
30. C. J. Allen, S. Mukerjee, E. J. Plichta, M. A. Hendrickson, and K. M. Abraham, "Oxygen Electrode Rechargeability in an Ionic Liquid for the Li–Air Battery." *The Journal of Physical Chemistry Letters*, **2**, 2420 (2011).
31. A. W. Lodge, M. J. Lacey, M. Fitt, N. Garcia-Araez, and J. R. Owen, "Critical appraisal on the role of catalysts for the oxygen reduction reaction in lithium-oxygen batteries." *Electrochimica Acta*, **140**, 168 (2014).
32. J. Herranz, A. Garsuch, and H. A. Gasteiger, "Using Rotating Ring Disc Electrode Voltammetry to Quantify the Superoxide Radical Stability of Aprotic Li–Air Battery Electrolytes." *The Journal of Physical Chemistry C*, **116**, 19084 (2012).
33. J. T. Frith, A. E. Russell, N. Garcia-Araez, and J. R. Owen, "An in-situ Raman study of the oxygen reduction reaction in ionic liquids." *Electrochemistry Communications*, **46**, 33 (2014).
34. T. Kuboki, T. Okuyama, T. Ohsaki, and N. Takami, "Lithium-air batteries using hydrophobic room temperature ionic liquid electrolyte." *Journal of Power Sources*, **146**, 766 (2005).
35. G. A. Elia, J. Hassoun, W. J. Kwak, Y. K. Sun, B. Scrosati, F. Mueller, D. Bresser, S. Passerini, P. Oberhumer, N. Tsiouvaras, and J. Reiter, "An advanced lithium-air battery exploiting an ionic liquid-based electrolyte." *Nano letters*, **14**, 6572 (2014).
36. M. Piana, J. Wandt, S. Meini, I. Buchberger, N. Tsiouvaras, and H. A. Gasteiger, "Stability of a Pyrrolidinium-Based Ionic Liquid in Li-O2 Cells." *Journal of the Electrochemical Society*, **161**, A1992 (2014).
37. N. Mozhzhukhina, L. P. Méndez De Leo, and E. J. Calvo, "Infrared Spectroscopy Studies on Stability of Dimethyl Sulfoxide for Application in a Li–Air Battery." *The Journal of Physical Chemistry C*, **117**, 18375 (2013).
38. J. P. Vivek, N. Berry, G. Papageorgiou, R. J. Nichols, and L. J. Hardwick, "Mechanistic Insight into the Superoxide Induced Ring Opening in Propylene Carbonate Based Electrolytes using in Situ Surface-Enhanced Infrared Spectroscopy." *Journal of the American Chemical Society*, **138**, 3745 (2016).
39. Vlad Zamlynny and Jacek Lipkowski. Quantitative SNIFTIRS and PM IRRAS of Organic Molecules at Electrode Surfaces. *In book: Advances in Electrochemical Science and Engineering: Diffraction and Spectroscopic Methods in Electrochemistry*, Wiley (2008), Volume 9, pp. 315.
40. T. Iwasita and F. C. Nart, "In situ infrared spectroscopy at electrochemical interfaces." *Progress in Surface Science*, **55**, 271 (1997).
41. H. Baltruschat, "Differential electrochemical mass spectrometry." *Journal of the American Society for Mass Spectrometry*, **15**, 1693 (2004).
42. H. A. E. A. Abd-El-Latif Baltruschat, *Electrochemical Mass Spectroscopy*. In Encyclopedia of Applied Electrochemistry, G. Kreysa, K.-i. Ota, and R. Savinell, Eds. Springer: New York 2014, 507−516.
43. P. C. Howlett, N. Brack, A. F. Hollenkamp, M. Forsyth, and D. R. MacFarlane, "Characterization of the Lithium Surface in N-Methyl-N-alkylpyrrolidinium Bis(trifluoromethanesulfonyl)amide Room-Temperature Ionic Liquid Electrolytes." *Journal of the Electrochemical Society*, **153**, A595 (2006).
44. K. Hanke, M. Kaufmann, G. Schwaab, M. Havenith, C. T. Wolke, O. Gorlova, M. A. Johnson, B. P. Kar, W. Sander, and E. Sanchez-Garcia, "Understanding the ionic liquid [NC4111][NTf2] from individual building blocks: an IR-spectroscopic study." *Physical Chemistry Chemical Physics*, **17**, 8518 (2015).
45. A. Lahiri, N. Borisenko, A. Borodin, M. Olschewski, and F. Endres, "Characterisation of the solid electrolyte interface during lithiation/delithiation of germanium in an ionic liquid." *Physical Chemistry Chemical Physics*, **18**, 5630 (2016).
46. O. Cheung, Z. Bacsik, Q. Liu, A. Mace, and N. Hedin, "Adsorption kinetics for CO_2 on highly selective zeolites NaKA and nano-NaKA." *Applied Energy*, **112**, 1326 (2013).
47. F. Nart and T. Iwasita, In situ FTIR as a Tool for Mechanistic Studies. Fundamentals and Applications. In *in Encyclopedia of Electrochemistry*; Wiley-VCH, Ed., 2003.
48. D. Lin-Vein, N. B. Colthup, W. G. Fateley, and J. G Grasselli, *The Handbook of Infrared and Raman Characteristic Frequencies of Organic Molecules*. In Academic Press, Inc. San Diego, CA, 1991.
49. I. Rey, P. Johansson, J. Lindgren, J. C. Lassègues, J. Grondin, and L. Servant, "Spectroscopic and Theoretical Study of (CF3SO2)2N- (TFSI-) and (CF3SO2)2NH (HTFSI)." *The Journal of Physical Chemistry A*, **102**, 3249 (1998).